AIP | Review of Scientific Instruments

Design challenges and analysis of the ITER core LIDAR Thomson scattering system

M. J. Walsh, M. Beurskens, P. G. Carolan, M. Gilbert, M. Loughlin, et al.

Citation: Rev. Sci. Instrum. **77**, 10E525 (2006); doi: 10.1063/1.2336473
View online: http://dx.doi.org/10.1063/1.2336473
View Table of Contents: http://rsi.aip.org/resource/1/RSINAK/v77/i10
Published by the American Institute of Physics.

Design challenges and analysis of the ITER core LIDAR Thomson scattering system

M. J. Walsh, M. Beurskens, P. G. Carolan, M. Gilbert, M. Loughlin, A. W. Morris, V. Riccardo, and Y. Xue
EURATOM/UKAEA Fusion Association, Culham Science Centre, Abingdon, Oxfordshire, OX14 3DB, United Kingdom

R. B. Huxford
RBH Optics, Burgess Hill, West Sussex RH15 8HL, United Kingdom

C. I. Walker
ITER International Team, Garching Joint Work Site, D-85746 Garching, Germany

(Received 5 May 2006; presented on 8 May 2006; accepted 16 July 2006; published online 19 October 2006)

The maximum temperature expected in ITER is in the region of 40 keV and the minimum average density of approximately 3×10^{19} m^{-3} is also expected. The proven capability, convenience, and port occupancy of the LIDAR Thomson scattering approach, demonstrated on JET, makes it an excellent candidate for ITER. Nonetheless, there are formidable design challenges in realizing such a diagnostic system. The expected high temperature presents its own problem of a very large relativistic blueshift of the scattered spectrum (e.g., $\lambda/\lambda_0\sim0.35$ for $T_e=40$ keV), impacting on the laser choice and spectrometer/detector system. The combination of coupling high power lasers to the plasma and broadband wavelength detection has been examined in terms of minimizing the operational risk to the overall system, while optimizing the diagnostic performance. Part of the exercise has also included identifying the present critical components, and reducing their impact, e.g., on diagnostic reliability and performance, and attempt to make the design compatible with possible long term developments and operational requirement. Issues such as redundancy of key operational components, e.g., lasers are explored. © *2006 American Institute of Physics.*
[DOI: 10.1063/1.2336473]

INTRODUCTION

The outline measurement requirements of the ITER core electron temperature and density diagnostics are shown in Table I. It is proposed to measure this with a LIDAR Thomson scattering system, with a laser beam injected approximately horizontally through an equatorial port. A possible outline design is shown in Figs. 1 and 2, indicating the laser beam directed towards the core plasma, and the optical labyrinth for the scattered light positioned inside the ITER port plug. The LIDAR concept has been successfully deployed at JET,[1] however, in ITER, a substantial part of the optics has to be in the vacuum vessel.

Key elements in the system implementation are control of the first mirror and collection window integrity across a large wavelength range and maintainability of the laser window under extended irradiation of neutrons and laser radiation. Technical developments in lasers and detectors are also important.

SCATTERED SPECTRUM

Some examples of the scattered spectra expected in ITER, including the substantial relativistic effects, are shown in Fig. 3.[2] It is clear that at the highest temperatures, the spectrum peaks significantly at shorter wavelengths.[3] To get to 40 keV at a scattering angle of 180° (LIDAR), one needs to measure down to $\lambda/\lambda_0\sim0.3-0.35$ (λ_0 is the laser wavelength). Typically, this extended region of the spectrum is problematic for high-optical transmission for both refractive and reflective components in the ITER environment due to the various effects of neutrons, gammas, and mirror degradation due to erosion or (mainly) deposition.

SPATIAL RESOLUTION

The spatial resolution specified are $a/30$ or $\delta x\sim7$ cm. This is at the limit of the present technology, particularly the combination of time resolution and the spectral range of detectors. The accuracy of the system will be ultimately limited by signal to background radiation and convoluting effects including those of laser pulse width and detector response time. Assuming that the temporal response of the system is given by the following: $\delta t=(c/2)(\delta x)$ where δt is the total convolved time response of the system including detector and laser. The total time of $\delta t\sim460$ ps is estimated to achieve the spatial resolution. Assuming Gaussian distributions and taking equal contributions from each of the components, a requirement is that the laser pulse and detector full width half maximum response times should be approximately 330 ps. Generally, the response time of the detectors

TABLE I. Main requirements for the core LIDAR.

	Spatial range	Parameter range	Time resolution	Space resolution	Accuracy
Electron Temperature	$r/a<0.9$	0.5-40 keV	10 ms	$a/30$	10%
Electron density	$r/a<0.9$	$3\times10^{19}-3\times10^{20}$ m^{-3}	10 ms	$a/30$	5%

is not Gaussian with the detectors having a slower fall time than rise time. This can be accounted for in the detailed analysis.

OPTICS

An outline scheme for the collection optics is shown in Fig. 2. In the case shown, the laser beam is injected through a hole in the first light collection mirror. This has the key advantage of separating the requirements for high power handling of the laser mirror from wide spectral bandwidth for the collection mirror, at the expense of a small hole in the collection mirror ($<5\%$ of total mirror area). The scattered light is relayed through a labyrinth to the vacuum window at the rear of the port plug. This arrangement while minimizing the direct escaping neutrons minimizes the neutron and debris load on the collection window. The etendue of the system will reduce with distance across the tokamak, with the minimum light being collected at the inner wall. The system indicated in Fig. 1 has a variation of f numbers from $\sim f/6$ at the outboard side to $f/18$ at the inner wall. This is compatible with collecting the light scattered from the whole cross section of the laser beam onto a single detector of diameter typical of available detectors although a twin detector approach for each spectral channel may be useful to minimize background light and optimize response time. These would allow the creation of a dual image plane to minimize the effects of depth of field. In this case, the first image which represents the light from the furthest away section of the plasma would be carefully extracted while almost all the remaining light (from the near field) would continue on to the second detector.

Rhodium is a good candidate for the reflection coating of the first collection mirror, although very little work has been carried out on its behavior in the ITER environment. It has a reasonable S-polarization reflectivity ($>75\%$) across the visible spectrum from 280 nm upwards. Locating the collection mirror further away from the plasma should help to reduce the impact of plasma interaction and hence increase the lifetime of this key component. In this design iteration, the first laser mirror is separated from the collection mirror and can be outside the vacuum. The first vacuum window is remote from the plasma. It is expected to be essentially immune from plasma deposition or erosion. As these are in the direct neutron path from the plasma, a study of the damage threshold of appropriately irradiated windows and mirrors with various wavelengths will need to be carried out. The arrangement shown has the advantage that the first laser mirror can be changed relatively easily without entering the area between the port plug back and the bioshield wall. The focusing lens for the laser beams could be installed in the stable bioshield wall. This would provide a solid mounting for the guiding laser optics and aid the system alignment. The vacuum pipe extension would need to be supported from the port plug.

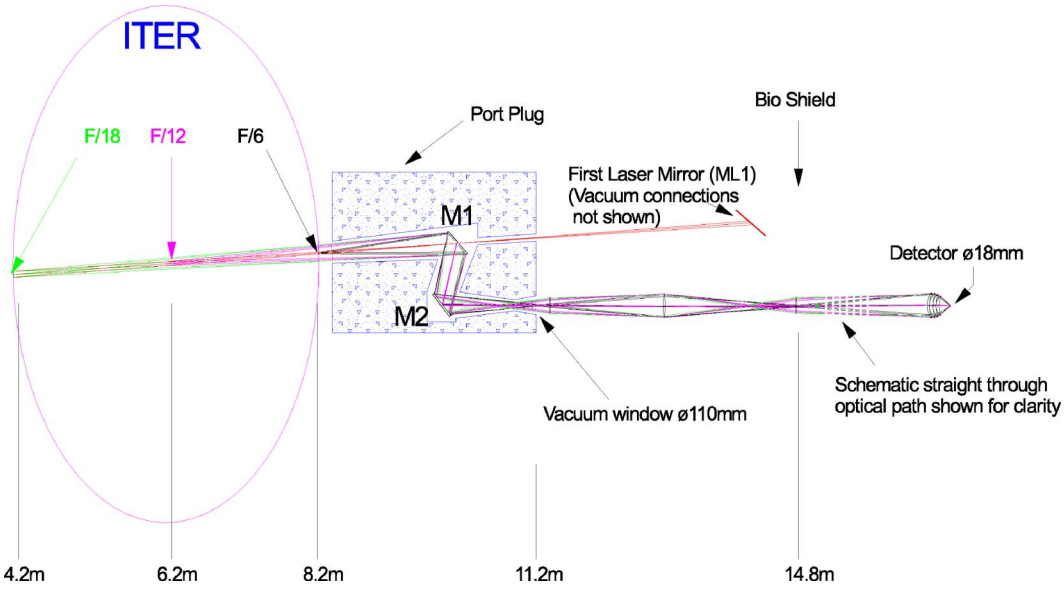

FIG. 1. (Color online) Generic arrangement for ITER core LIDAR. The light collection and the laser injection are separated.

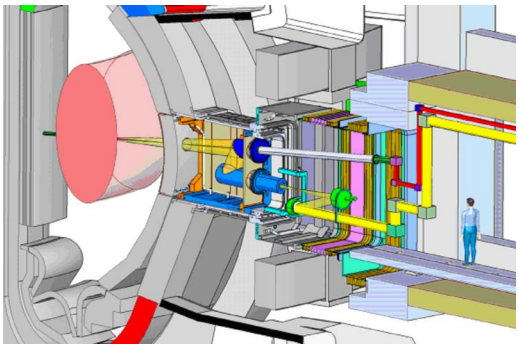

FIG. 2. (Color online) Outline schematic of the port plug area LIDAR design for ITER.

DETECTOR OPTIONS

The detectors under consideration at present are photomultiplier tube–microchannel plate (PMT-MCP) type. These have a relatively large aperture, >10 mm, and are responsive across the spectrum from 300 nm to approximately 800 nm using certain types of photocathodes such as GaAs, S20, and GaAsP. S20 based devices have adequate time response with full width at half maximum (FWHM) response times under 200 ps. However, S20 is relatively insensitive at the longer wavelengths (>680 nm) compared to the other photocathodes mentioned. The response times of these detectors are currently under investigation. Existing detectors are not adequate to allow a system based on first harmonic (Neodymium-yttrium aluminum garnet) Nd:YAG lasers to be used solely. Presently, the use of this laser would be confined to measuring temperatures greater than approximately 2.5 keV and hence it would need to be combined with a shorter wavelength laser (such as titanium: sapphire or second harmonic Nd:YAG). In the final detector solution, it is likely that several detector types will be utilized, each one optimized for different spectral regions.

LASER OPTIONS

The ITER specifications of 100 Hz laid down for the laser repetition rate can be achieved by going for a multilaser approach.[4] This will build in redundancy, allow a burst mode

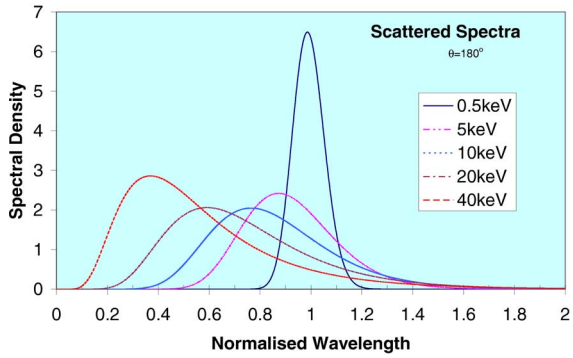

FIG. 3. (Color online) Example of the spectral intensity (arbitrary units) for 500 eV electron temperature compared with spectra for 5, 10, 20, and 40 keV plotted vs normalized wavelength with depolarization (λ/λ_0). To measure 40 keV a value of the order of 0.3–0.35 should be reached with the measurement apparatus. This would mean getting down to below 300 nm for an 800 nm laser or 400 nm for 1064 nm laser.

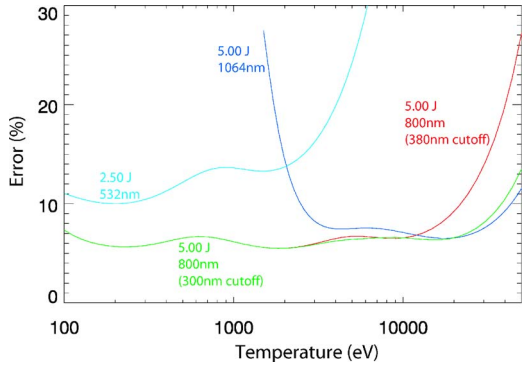

FIG. 4. (Color online) Typical error estimates expected for core (collection f number of 12) measurements.

option, and make the requirements realizable. Energies from the laser of the order of 5 J (FWHM <250 ps) are required. A system with approximately 15 Hz is feasible based on current technology. As reliability and availability are critical for ITER and as lasers are typically high maintenance items, maintenance needs to be considered as a design driver. Deciding on the exact number of lasers may be a financial or space issue but arrangements of lasers with certain symmetries are more appropriate. A triangular arrangement (three lasers set at corners of an equilateral triangle) or a hexagonal arrangement (seven lasers, six centered at the corner points of the hexagon and one in the core) is considered. For the seven laser case, each of these laser beams would be between 70 and 100 mm in diameter at the first laser mirror or the input window. The whole array would require an entrance window of approximately 170–200 mm in diameter. The size of the beams can be much smaller in the laser generating room where they are combined, hence minimizing the footprint of the laser array on the first laser mirror. It should be noted that the limiting vacuum aperture in the laser flight path would be the hole in the first collection mirror. This would be less than ~100 mm. This arrangement would also allow optimization of the laser beam size at the inner wall.

ERROR ANALYSIS

The expected performance of the LIDAR system is shown in Fig. 4 for a range of different potential laser options at the core of the plasma. In this case, the density is 3×10^{19} m^{-3}, $Z_{\text{eff}}=2$, and background enhancement over bremsstrahlung is estimated at 2. The cutoff wavelength for all lasers is 380 nm except where shown. The transmission of the laser to the target is estimated at 50% and the collection of the light from the target is 11%. The efficiency of the detectors is typically set at and average value of 3% at wavelengths below 550 nm and an average of 4% above this value. For the region above 800 nm, the average efficiency was set to 0.2%. These are consistent with typical detectors available at this time. An 18 mm detector area is assumed and the collection f number is 0.7 at this point. The spatial extent is 7 cm. The energy for the 532 nm laser was set at 50% of the 1064 nm, in line with second harmonic conversion efficiencies. The fractional error represents one standard deviation. To simulate the effect of extending the wavelength

region past the irradiation cutoff, one case has an extended wavelength down to 300 nm. The effect of doing this is seen in the figure. Based on the current assumptions, it is seen that a system to measure the core temperatures to better that 10% is outlined.

NEUTRON FLUX AND POWER LOADS ON COMPONENTS

Neutron loads on components in the port plug and cryostat area have been estimated for 500 MW of fusion power. The estimated neutron heating power on the first collection mirror is $\sim 17\ \mathrm{mW/cm^3}$ (Cu) ($7\times10^{11}\ n/\mathrm{cm^2\,s}$). The heating power at the second collection mirror is below $100\ \mu\mathrm{W/cm^3}$ ($\sim 4\times10^{9}\ n/\mathrm{cm^2\,s}$). At the first collection window, the power is negligible and the estimated neutron flux is in the region of $10^{8}\ n/\mathrm{cm^2\,s}$. The spectrum of neutrons that arrives at this window has energies typically below 1 MeV. These calculations assume a 60%/40% (volumetric ratio) of stainless steel/water mix distributed inside the walls of the plug. The neutron flux at the first laser mirror is estimated to be $\sim 10^{10}\ n/\mathrm{cm^2\,s}$.

According to the 2002 ITER design guidelines, the maximum radiative load (P_w) on the first wall during operation is $0.5\ \mathrm{MW/m^2}$.[5] Assuming that the aperture in the blanket has an area A ($\sim 0.07\ \mathrm{m^2}$) and the mirror is presenting an area B ($\sim 0.12\ \mathrm{m^2}$) at a distance L from the first wall (~ 2.35 m), then the power reaching the mirror is approximately, $P_{\mathrm{mirror}}=P_w(A/2\pi)(B/L^2)$, leading to a power of 130 W or a power density of $\sim 1\ \mathrm{kW/m^2}$ on the first mirror.

THERMOMECHANICAL ANALYSIS OF FIRST MIRROR

Using the above data, it is possible to estimate the effect of the heat sources on the first mirror. This analysis was carried out for a copper mirror substrate in good thermal contact with a stainless-steel supporting structure. The stainless steel was cooled. When the water temperature rise between the inlet and outlet is allowed to change up to 3°, the time-average mirror surface temperature has a maximum of $\sim 14.5\ ^{\circ}\mathrm{C}$ above ambient. The effect of the temperature on the surface profile is examined by calculating the change in the radius of curvature of the mirror across the mirror. The maximum curvature change is equivalent to a radius of ~ 1000 m. An option to keep the mirror at a temperature well above the $100\ ^{\circ}\mathrm{C}$ operating point of ITER is being considered to minimize deposition and keep the mirror clean.

TESTING AND IMPLEMENTATION

Implementation of a scattering system involves the use of high power lasers and generally requires isolation of the tokamak facility for safety reasons during the testing and commissioning. This time could be significantly reduced by creating a test rig that mimics as closely as possible the ITER geometry. This facility would also allow for testing of alignment systems, minimization of straylight (especially in the region between the first collection mirror and the end of the blanket shield module) and *in situ* calibration techniques to be developed and perfected. Some components such as the first laser window would need to be irradiated to test properly.

ACKNOWLEDGMENTS

This work is funded jointly by the U.K. Engineering and Physical Sciences Research Council and EURATOM, and undertaken as part of an EFDA Task. The authors are indebted to the Culham team and, in particular, to N. H. Balshaw, M. Dunstan, M. J. Forrest, D. Hare, K. Hawkins, M. Kempenaars, P. Parsons, R. Scannell, and G. Razdobarin for their contributions.

[1] H. Salzmann, K. Hirsch, P. Nielsen, C. Gowers, A. Gadd, M. Gadeberg, H. Murmann, and C. Schrödter, Nucl. Fusion **27**, 1925 (1987).
[2] O. Naito, H. Yoshida, and T. Matoba, Phys. Fluids B **5**, 4256 (1993) [O. Naito, H. Yoshida, and T. Matoba, Phys. Plasmas **1**, 806 (1994) (errata)].
[3] I. Hutchinson, *Principles of Plasma Diagnostics*, 2nd ed. (Cambridge University Press, Cambridge, 2002), Chap. 7.
[4] M. J. Walsh *et al.*, Rev. Sci. Instrum. **75**, 3909 (2004).
[5] A. E. Costley, T. Sugie, G. Vayakis, and C. I. Walker, Fusion Eng. Des. **74**, 109 (2005).